

NJC

Accepted Manuscript



This article can be cited before page numbers have been issued, to do this please use: M. Sutradhar, L. M. Martins, T. Roy Barman, M. L. Kuznetsov, M. F. C. Guedes da Silva and A. J. L. Pombeiro, *New J. Chem.*, 2019, DOI: 10.1039/C9NJ00348G.



This is an Accepted Manuscript, which has been through the Royal Society of Chemistry peer review process and has been accepted for publication.

Accepted Manuscripts are published online shortly after acceptance, before technical editing, formatting and proof reading. Using this free service, authors can make their results available to the community, in citable form, before we publish the edited article. We will replace this Accepted Manuscript with the edited and formatted Advance Article as soon as it is available.

You can find more information about Accepted Manuscripts in the [author guidelines](#).

Please note that technical editing may introduce minor changes to the text and/or graphics, which may alter content. The journal's standard [Terms & Conditions](#) and the ethical guidelines, outlined in our [author and reviewer resource centre](#), still apply. In no event shall the Royal Society of Chemistry be held responsible for any errors or omissions in this Accepted Manuscript or any consequences arising from the use of any information it contains.

Vanadium complexes of different nuclearities in the catalytic oxidation of cyclohexane and cyclohexanol – An experimental and theoretical investigation

Manas Sutradhar,* Luísa M.D.R.S. Martins,* Tannistha Roy Barman, Maxim L. Kuznetsov,* M. Fátima C. Guedes da Silva and Armando J. L. Pombeiro*

Centro de Química Estrutural, Instituto Superior Técnico, Universidade de Lisboa, Av. Rovisco Pais, 1049-001 Lisboa, Portugal

Email: manas@tecnico.ulisboa.pt (MS); luisamargaridamartins@tecnico.ulisboa.pt (LMDRSM); max@mail.ist.utl.pt (MLK); pombeiro@tecnico.ulisboa.pt (AJLP)

Abstract

The mono-, bi- and tri-nuclear oxidovanadium(V) complexes $[\text{VO}(\text{OEt})(\text{L}^1)]$ (**1**), $[\{\text{VO}(\text{OEt})(\text{EtOH})\}_2(\text{L}^2)]$ (**2**) and $[\{\text{VO}(\text{OMe})(\text{H}_2\text{O})\}_3(\text{L}^3)] \cdot 2\text{H}_2\text{O}$ (**3**) ($\text{L}^1 = 2$ -hydroxy-(2-hydroxybenzylidene)benzohydrazide, $\text{L}^2 = \text{bis}(2$ -hydroxybenzylidene)terephthalohydrazide and $\text{L}^3 = \text{tris}(2$ -hydroxybenzylidene)benzene-1,3,5-tricarbohydrazide) (**3** was synthesized for the first time) were used to investigate the role of vanadium nuclearity in the catalytic oxidation of cyclohexane and cyclohexanol. They are active homogeneous catalysts for the microwave-assisted neat peroxidative oxidation of cyclohexane (with aq. H_2O_2 to cyclohexanol and cyclohexanone) and cyclohexanol (with aq. $t\text{BuOOH}$ to cyclohexanone). A mechanism of the HO^\bullet radical generation – the rate limiting step of the cyclohexane oxidation by H_2O_2 – was investigated in detail by theoretical DFT methods. The mechanism is different from those usually accepted for the Fenton or Fenton-like systems and it includes (i) coordination of H_2O_2 to the catalyst molecule, (ii) proton transfer from ligated H_2O_2 to the methoxy ligand and elimination of the formed methanol molecule and (iii) coordination of the second H_2O_2 molecule followed by HO-OH bond cleavage to give HO^\bullet . The activation of the ligated H_2O_2 towards this cleavage is associated with the redox active nature of the ligand L in the catalyst molecule, which acts (instead of the metal) as the reducing agent of the H_2O_2 ligand.

Keywords: Oxidovanadium(V) complexes; aroylhydrazone; microwave-assisted oxidation; DFT calculations; Mechanism.

Introduction

The oxidation of alkanes is receiving special attention as hydrocarbons of this type are cheap and abundant in nature and can be important as potential precursors for the synthesis of useful products.¹⁻¹⁸ However, the oxidation of alkanes is highly challenging due to their inertness, and their activation for such processes is rather difficult. Also, the selective oxidation of alcohols to afford carbonyl compounds is recognized as a key reaction in synthetic organic chemistry.¹⁹⁻²³ In view of economic and environmental reasons, the development of efficient and selective catalysts for such oxidation reactions under sustainable conditions is challenging. The use of microwave irradiation to assist such reactions can contribute to that aim, on account of its simplicity, accelerating power and energy saving.²²⁻²⁴

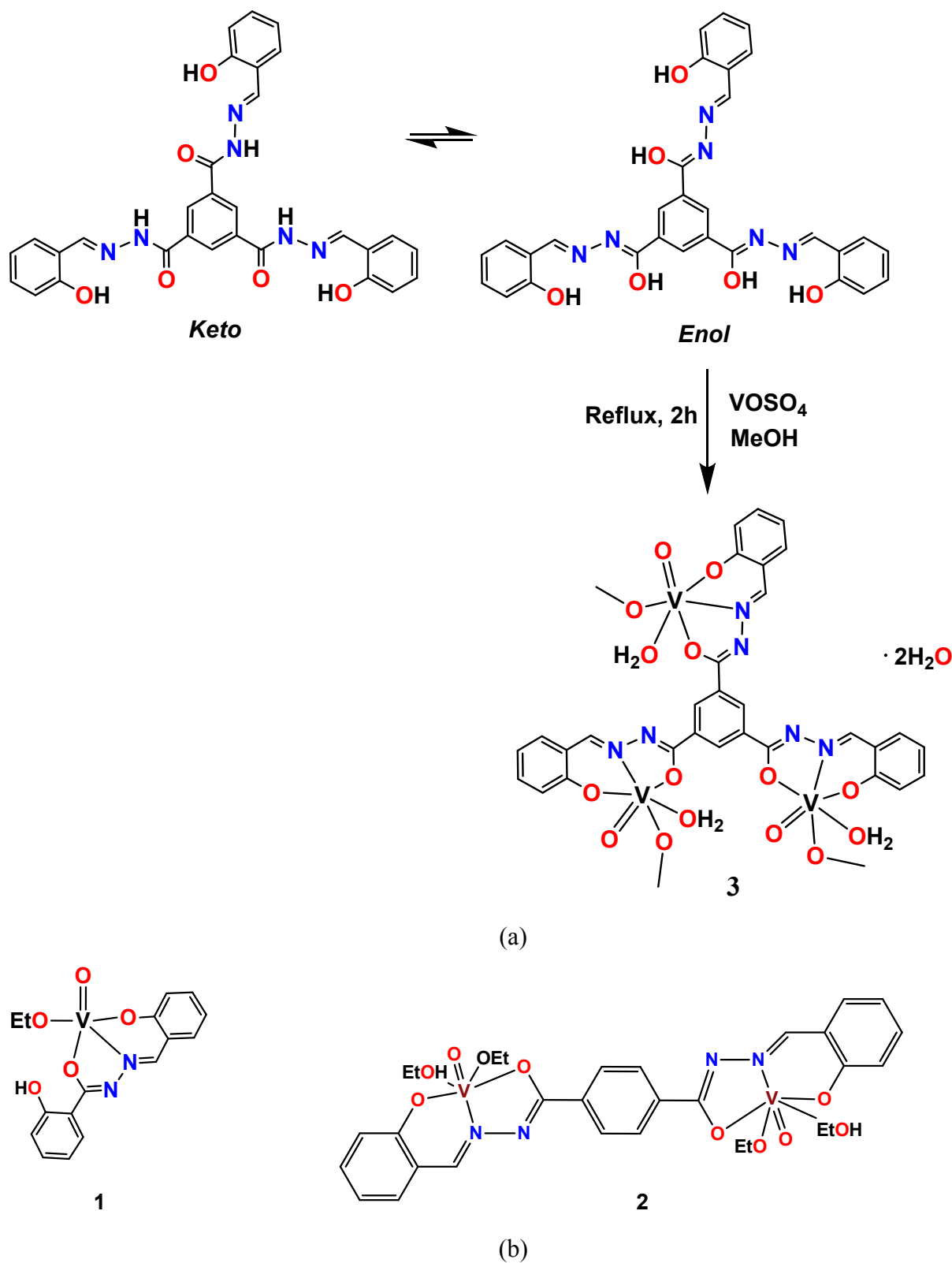
The role of vanadium in the development of oxidation catalysts has been object of current and growing interest from both biological and chemical perspectives.^{1-8,25,26} They catalyze various C-H oxidation reactions of organic substrates, *e.g.*, saturated, aromatic, and olefinic hydrocarbons by H₂O₂ and some other organic peroxides (for example, *tert*-butyl hydroperoxide, TBHP).²⁷ Vanadium complexes have also shown potential as active catalysts for oxidation of alcohols in the presence of suitable stoichiometric oxidants like H₂O₂, TBHP or dioxygen.¹⁻⁸

In continuation of our interest in designing metal complexes derived from aroyhydrazones to catalyze oxidation reactions²⁸⁻³⁷ herein we report the catalytic activities of three oxidovanadium(V) complexes with three different nuclearities (mono, bi and tri) having a similar type of azine based ligands towards the microwave assisted oxidation of alkanes and alcohols under mild conditions. The mono and binuclear complexes [VO(OEt)(L¹)] (**1**) and [{VO(OEt)(EtOH)}₂(L²)] (**2**) have been synthesized according to the literature.^{28,38,39} The synthesis of multidentate N,O donor azine based ligand having three coordination pockets, tris(2-hydroxybenzylidene)benzene-1,3,5-tricarbohydrazide (H₆L³) and of its trinuclear oxidovanadium(V) complex [{VO(OMe)(H₂O)}₃(L³)]·H₂O (**3**) are reported for the first time in this study. The catalytic activities of these complexes having three different nuclearities towards the solvent-free microwave-assisted oxidation of cyclohexane and cyclohexanol are explored by experimental and theoretical DFT studies, to propose a possible mechanistic pathway of the catalytic peroxidative oxidation of cyclohexane.

Results and discussion

Three aroylhydrazone ligands having similar coordinating moieties but differing in their number have been used to synthesize the oxidovanadium(V) complexes **1-3** with different nuclearities. Complexes **1** and **2** have been synthesized according to a reported method.^{28,38,39} To prepare a trinuclear oxidovanadium(V) complex having a tris-tridentate aroylhydrazone moiety the pro-ligand tris(2-hydroxybenzylidene)benzene-1,3,5-tricarbohydrazide (H_6L^3) has been synthesized (see experimental) and used. This tris(aroylhydrazone) behaves as a potentially nonadentate ligand. It undergoes enolization in solution can act as a tris(di-negative) chelator (Scheme 1) being able to simultaneously encapsulate three metal ions. Its reaction with $VOSO_4$ in methanol led to the formation of the trinuclear oxidomethoxidovanadium(V) complex $[\{VO(OMe)(H_2O)\}_3(L^3)] \cdot 2H_2O$ (**3**) (Scheme 1). The oxidation of the oxidovanadium(IV) moiety to the oxidovanadium(V) species in solution under aerobic conditions is well known.^{4,28,29,32,33,38-41}

The characterization of complex **3** has been carried out by elemental analysis, IR and NMR (1H , ^{51}V) spectroscopy, ESI-MS and single crystal X-ray diffraction. The IR spectrum of complex **3** displays the $\nu(O-H)$ bands of coordinated and non-coordinated water molecules at 4218 and 4061 cm^{-1} , the $\nu(C=N)$ band at 1602, the enolic $\nu(C-O)$ band at 1250 and $\nu(N-N)$ band at 1036 cm^{-1} . Three characteristic $\nu(V=O)$ bands are observed at 1007, 986 and 914 cm^{-1} , which are the signature of oxidovanadium(IV) and (V) compounds.^{4,28,29,32,33,38-41} In the ESI-MS spectrum, the m/z value indicates the presence of the trinuclear species with the loss of two water molecules (see Experimental). The 1H NMR spectrum shows the aromatic protons in the range δ 7.65- δ 6.94, the benzylic protons at δ 8.62 and a broad signal of methyl protons of the methoxido groups at δ 3.72. The presence of three oxidovanadium centres is observed at -529, -541 and -579 ppm in the ^{51}V NMR spectrum. The UV-Vis spectra of **1-3** have been recorded in acetonitrile and also under catalytic reaction conditions (Fig. S1, supporting information). From these spectra it can be assumed that the complexes form new species in the presence of H_2O_2 , therefore being better considered as catalytic precursors than catalysts. The speciation and reactivity of metal complexes in solution⁴²⁻⁴⁴ is therefore important to identify reacting species, what concerns a future work. The X-ray crystal structure of **3** is described below.



Scheme 1 (a) Synthesis of $[\{\text{VO}(\text{OMe})(\text{H}_2\text{O})\}_3(\text{L}^3)] \cdot 2\text{H}_2\text{O}$ (**3**); (b) Structures of **1** and **2**.

Description of Crystal Structure

X-ray quality crystals of **3** were obtained upon slow evaporation of a methanol solution of the compound, at room temperature. Fig. 1 displays a perspective view of the molecule, crystallographic data are summarized in Table 1 and selected dimensions are presented in Table 2.

The hexaanionic ligand (L^3)⁶⁻ acts as tris(tridentate) N_3O_6 chelating species towards three vanadium cations. Each metal displays distorted N_1O_5 octahedral environment with the basal plane engaged with the O-phenolic, the O-enolic and the N-imine atoms of the chelating ligand and with an O-methoxide. The axial positions are occupied by the O-oxido and the O-water molecule. Considering the least square (l.s.) planes constructed with the equatorial binding atoms, the metal cations are situated 0.309 (V1), 0.314 (V2) and 0.274 Å (V3) towards the corresponding oxido atom.

Various structural parameters in **3** are in agreement with those already reported.^{4,28,29,32,33,38-45} Thus, the $O_{\text{oxido}}-V-O_{\text{methoxide}}$ bond angles assume values of 173.0(3)°, 174.1(3)° and 176.1(3)°, but those involving the chelator O-atoms adopt values of 150.8(3)°, 151.6(3)° and 152.6(2)° because of chelation constrains and justify the observed octahedral distortion. The average N-V-O angles in the five- and six-membered metallacycles are of 74.3(2) and 83.6(2)°, respectively. The V=O and V-O_{water} bond distances average 1.555(6) and 2.303(7) Å, respectively. The various vanadium-oxygen bond lengths in **3** follow the order $V-O_{\text{oxido}} < V-O_{\text{methoxido}} < V-O_{\text{phenoxido}} < V-O_{\text{enolate}} < V-O_{\text{water}}$.

Considering the least-square plane that contains the vanadium cations (the V-plane), the coordinated water molecules are all on the same side of that plane, together with the central aromatic ring of (L^3)⁶⁻ whose l.s. plane is twisted, relatively to the V-plane, by 3.36°. The phenolate rings bound to V2 and V3 also incline to that side of the V-plane, their l.s. planes making angles of 7.95° and 10.66°, in this order, with the latter. The phenolate ring bound to V1, however, is displaced to the opposite side by 22.13°.

In view of the number of water molecules in the structure, the molecules of **3** are involved in several medium intense H-bond interactions that give rise to an infinite 2D network with base vectors [010] and [101]. The minimum intramolecular $V \cdots V$ distance is of 9.417 Å, but the intermolecular one is considerably shorter, 5.970 Å, and comprises the V2 and V3 cations.

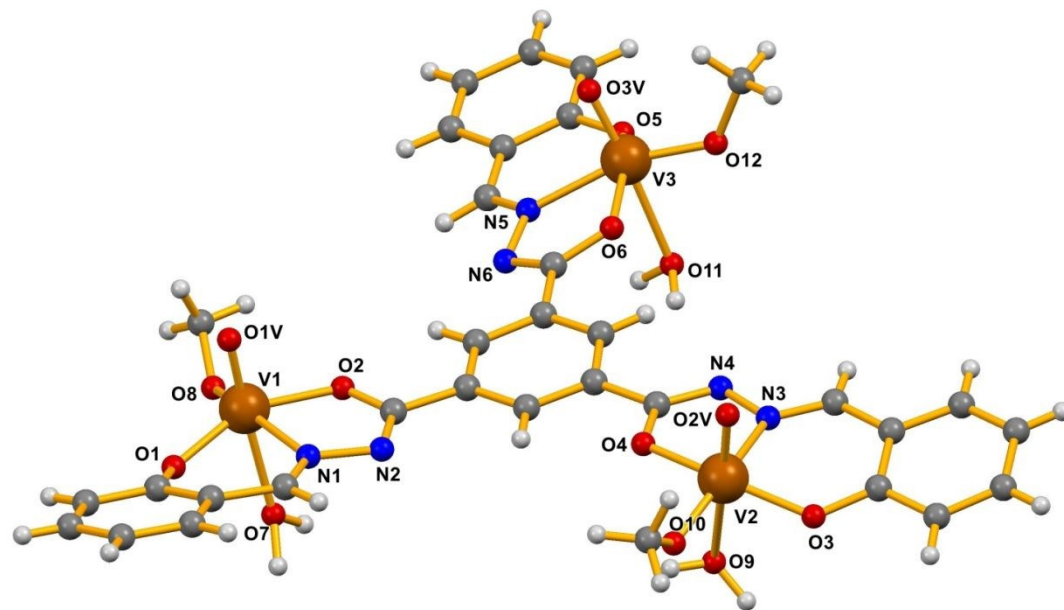


Fig. 1 Molecular structure of $[\{VO(OMe)(H_2O)\}_3(L^3)] \cdot 2H_2O$ (**3**) with partial atom numbering scheme. Solvated water molecule is omitted for clarity.

Table 1. Crystal data and structure refinement details for complex **3**.

Empirical formula	$C_{33}H_{33}N_6O_{15}V_3 \cdot 2H_2O$
Formula Weight	942.49
Crystal system	Triclinic
Space group	<i>P</i> -1
<i>a</i> /Å	11.6728 (12)
<i>b</i> /Å	13.1012 (12)
<i>c</i> /Å	13.9688 (12)
α /°	98.888 (5)
β /°	111.434 (4)
γ /°	92.418 (5)
<i>V</i> (Å ³)	1953.3 (3)
<i>Z</i>	2
<i>D</i> _{calc} (g cm ⁻³)	1.572
μ (Mo <i>K</i> α) (mm ⁻¹)	0.782
Rfls. collected/unique/observed	21572/6755/3185
<i>R</i> _{int}	0.0793
Final <i>R</i> 1 ^a , <i>wR</i> 2 ^b (<i>I</i> ≥ 2σ)	0.0880, 0.1849
Goodness-of-fit on <i>F</i> ²	1.044

$$^a R = \sum ||F_o| - |F_c|| / \sum |F_o| ; ^b wR(F^2) = [\sum w(|F_o|^2 - |F_c|^2)^2 / \sum w|F_o|^4]^{1/2}$$

Table 2. Selected parameters, bond distances (Å) and angles (°) in complex **3**.

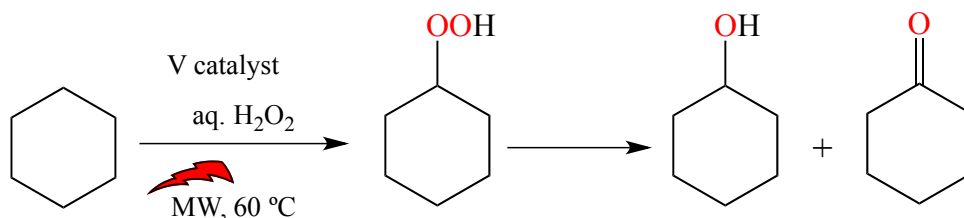
O1—V1	1.849(6)	O4—V2	1.934 (5)	O8—V1	1.762(6)
O1V—V1	1.557(6)	O3V—V3	1.612(6)	O9—V2	2.343(7)
O2—V1	1.932(5)	O5—V3	1.814(6)	O10—V2	1.760(6)
O2V—V2	1.583(6)	O6—V3	1.921(5)	O11—V3	2.336(8)
O3—V2	1.834(6)	O7—V1	2.292(6)	O12—V3	1.759(6)

O1V—V1—O8	104.0 (3)	O2V—V2—O10	102.3 (3)	O3V—V3—O12	99.3 (3)
O1V—V1—O1	99.4 (3)	O2V—V2—O3	101.7 (3)	O3V—V3—O5	99.8 (4)
O8—V1—O1	103.5 (3)	O10—V2—O3	100.6 (3)	O12—V3—O5	103.2 (3)
O1V—V1—O2	98.1 (3)	O2V—V2—O4	98.5 (3)	O3V—V3—O6	99.6 (3)
O8—V1—O2	92.4 (3)	O10—V2—O4	95.4 (3)	O12—V3—O6	93.8 (3)
O1—V1—O2	152.6 (2)	O3—V2—O4	150.8 (3)	O5—V3—O6	151.6 (3)
O1V—V1—N1	94.1 (3)	O2V—V2—N3	94.2 (3)	O3V—V3—N5	94.2 (3)
O8—V1—N1	159.0 (3)	O10—V2—N3	161.7 (3)	O12—V3—N5	163.5 (3)
O1—V1—N1	83.6 (3)	O3—V2—N3	83.6 (2)	O5—V3—N5	83.7 (3)
O2—V1—N1	74.3 (2)	O4—V2—N3	74.1 (2)	O6—V3—N5	74.4 (2)
O1V—V1—O7	174.1 (3)	O2V—V2—O9	173.0 (3)	O3V—V3—O11	176.1 (3)
O8—V1—O7	81.8 (3)	O10—V2—O9	82.9 (3)	O12—V3—O11	84.1 (3)
O1—V1—O7	79.6 (3)	O3—V2—O9	81.7 (3)	O5—V3—O11	81.1 (3)
O2—V1—O7	80.8 (2)	O4—V2—O9	76.2 (2)	O6—V3—O11	78.2 (3)
N1—V1—O7	80.0 (2)	N3—V2—O9	80.0 (2)	N5—V3—O11	82.1 (3)

Catalysis

Following our attempt^{28,29,32} of using oxidovanadium(V) complexes to catalyze the oxidation of cyclohexane with aqueous hydrogen peroxide usually in NCMe at room temperature, herein compounds **1–3** were successfully tested as homogeneous catalysts for the microwave-assisted neat oxidation (without added solvent) of cyclohexane with aq. hydrogen peroxide to cyclohexanol and cyclohexanone. Cyclohexyl hydroperoxide (CyOOH) is formed as a primary product and evolves in a mixture of cyclohexanol and cyclohexanone (final products, Scheme 2). The formation of CyOOH was proved by using Shul'pin's method^{8,46–48} (see experimental): the addition of PPh₃ prior to the GC analysis of the products resulted in a marked increase of the amount of cyclohexanol (due to the reduction of CyOOH by PPh₃ and formation of phosphine oxide) and decrease in the amount of cyclohexanone relatively to those of the sample not subjected to the reduction (see Table 3, entry 14

versus entry 12). The product yields given in Table 3 (except if indicated otherwise) were obtained upon addition of PPh₃, where A concerns the total of cyclohexanol + CyOOH at the end of the catalytic reaction.



Scheme 2 MW-assisted neat oxidation of cyclohexane to cyclohexyl hydroperoxide, cyclohexanol and cyclohexanone with aqueous hydrogen peroxide catalysed by **1–3**.

Under the optimized eco-friendly conditions of these solvent- and additive-free systems (60 °C and 1.5 h of low power (25 W) MW irradiation), yields up to 39% (for the trinuclear complex **3**, entry 12 of Table 3) of the oxygenated products are obtained (Scheme 2, Fig. 2) using a low vanadium catalyst load (0.2% molar ratio relatively to cyclohexane). This yield value is *ca.* 5 times higher than the best ones (8%) reported^{49,50} for the industrial aerobic process to assure a good selectivity. Cyclohexanol and cyclohexanone were the only products detected by GC-MS analysis under these assayed conditions, thus revealing a very selective oxidation system. The reaction proceeds very quickly, in accord with a high activity of our V catalysts. In fact, after only 15 min of MW irradiation 15 (**1**), 23 (**2**) and 26% (**3**) yield of oxygenates are achieved (Table 3, entries 1, 5 and 9, respectively).

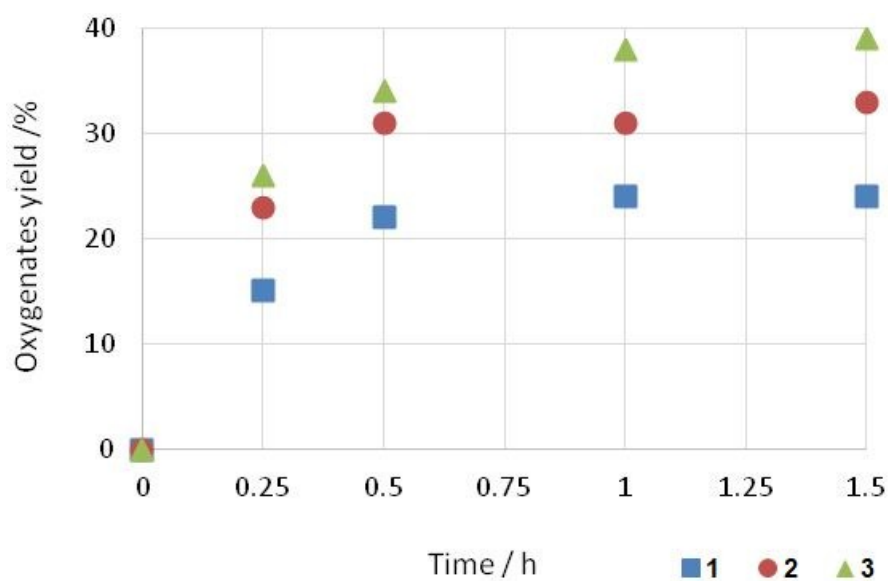


Fig. 2 Effect of the reaction time on the total yield of cyclohexanol and cyclohexanone obtained by microwave-assisted neat oxidation of cyclohexane with H_2O_2 catalyzed by complexes **1–3**.

Table 3. Selected data^a for the MW-assisted oxidation of cyclohexane with H_2O_2 catalysed by **1 - 3**.

Entry	Catalyst	Time / h	Yield / % ^b		Total	A/K ^c	Total TON ^d	Total TOF / h ^{-1 e}
			Cyclohexanol + CyOOH (A)	Cyclohexanone (K)				
1	1	0.25	10.1	4.9	15	2.1	75	300
2		0.5	17.4	6.6	24	2.6	110	220
3		1.0	16.9	7.1	24	2.4	120	120
4		1.5	15.8	8.2	24	1.9	120	80
5	2	0.25	17.8	5.2	23	3.4	115	460
6		0.5	24.3	6.7	31	3.6	155	310
7		1.0	24.9	6.3	31	4.0	155	155
8		1.5	24.2	8.8	33	2.8	165	110
9	3	0.25	19.2	6.8	26	2.8	130	520
10		0.5	27.6	6.4	34	4.3	170	340
11		1.0	32.2	5.8	38	5.6	190	190
12		1.5	32.8	6.2	39	4.8	190	127
13 ^f		1.5	0.6	0.5	1	1.2	6	4
14 ^g		1.5	14.8	12.2	27	1.2	135	90
15 ^h		1.5	26.4	4.6	31	5.8	21	14
16 ⁱ	-	1.5	0.1	0.0	0.1	-	-	-
17	VOSO_4	1.5	2.1	0.9	3	2.3	15	10
18	$[\text{VO}(\text{acac})_2]$	1.5	5.8	1.2	7	4.8	35	23

^aReaction conditions (unless stated otherwise): CyH (2.5 mmol), aq. H₂O₂ (5.0 mmol), 5.0 μmol of **1** - **3** (0.2 mol% vs. CyH), 60 °C, 0.25 – 1.5 h of MW irradiation. Yields and TONs determined by GC analysis (upon treatment with PPh₃). ^bPercentage molar yield (moles of product per mole of cyclohexane); values obtained upon addition of PPh₃ (see experimental). ^cRatio between the molar concentrations of A and K. ^dTotal turnover number = moles of A and K *per* mol of catalyst. ^eTOF=TON *per* hour. ^fIn the presence of NHPPh₂. ^gWithout PPh₃ treatment. ^hUnder N₂ atmosphere. ⁱWithout catalyst.

The effect of MW radiation (that generates heat evenly throughout the reactor) on the catalytic performance of **3** was evaluated by comparison with the use of the conventional heating (oil bath) and is shown in Fig. 3. For the same reaction conditions (including reaction time), the catalytic activity was always strongly enhanced by MW irradiation, while selectivity for the KA oil was preserved until 1.5 h reaction time. For longer reaction periods, under MW irradiation, small amounts of byproducts such as 1,2- and 1,4-cyclohexanediols were detected by GC-MS analysis in the final reaction mixtures with the concomitant slight decrease of KA oil yield (Fig. 3).

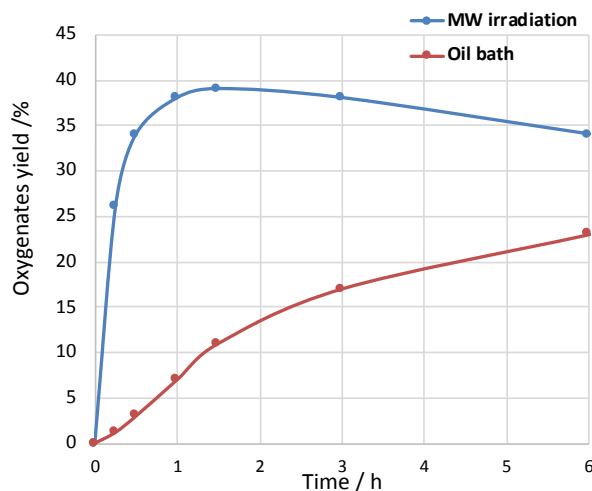
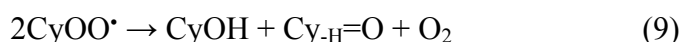
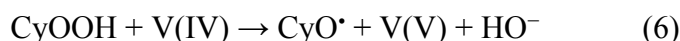


Fig. 3 Effect of the heating mode (MW irradiation or oil bath) on the total yield of cyclohexanol and cyclohexanone obtained by neat oxidation of cyclohexane with aq. H₂O₂ catalyzed by complex **3**.

Thus, the use of MW radiation as alternative energy source is appealing for the present catalytic system, enhancing product yield as well as being more energy efficient and economical in comparison to the conventional oil bath heating method. The catalytic performance found for the present V-systems is much better than those previously observed³² for the oxidovanadium(V)

1
2 aroylhydrazone complexes [VOL¹(OEt)]·[VOL¹(OEt)(EtOH)], [VOL²(OEt)], [Et₃NH][VO₂L¹],
3 [VO₂(HL²)]·2EtOH, [(VOL¹)₂(μ-O)] or [(VOL²)₂(μ-O)] (0.6 - 1.7% KA oil yield).
4
5

6 Addition of a radical trap (*e.g.*, Ph₂NH) to the reaction mixture results in almost suppression
7 of the catalytic activity of **3** (Table 3, entry 13). This behaviour, along with the formation of
8 cyclohexyl hydroperoxide (typical intermediate product in radical-type reactions) supports the
9 hypothesis of a free-radical mechanism for the cyclohexane oxidation carried out in this study,
10 similarly to the reported for other vanadium-catalyzed oxidations of cyclohexane by hydrogen
11 peroxide.^{28,29,51-53} The V-assisted decomposition of H₂O₂ leading to the oxygen-centred radicals
12 HOO• and HO• (reactions 1 and 2) can be proposed (see Scheme 3). Cyclohexyl radical (Cy•) is then
13 formed upon H-abstraction from cyclohexane (CyH) by HO• (reaction 3). Reaction of Cy• with O₂
14 leads to CyOO• (reaction 4), and CyOOH can then be formed *e.g.*, upon H-abstraction from H₂O₂ by
15 CyOO• (reaction 5). Vanadium complex-assisted decomposition of CyOOH to CyO• and CyOO•
16 (reactions 6 and 7) would then lead to cyclohexanol (CyOH) and cyclohexanone (Cy_{-H}=O) products
17 (reactions 8 and 9).⁵¹⁻⁵⁵
18
19
20
21
22
23
24
25
26
27
28
29
30
31
32
33
34
35
36
37
38
39
40
41
42
43
44
45
46
47

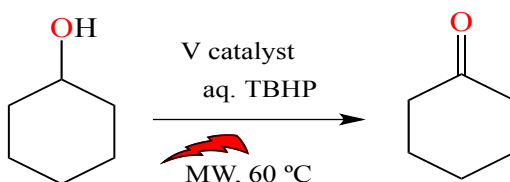


48 **Scheme 3** free-radical mechanism for the cyclohexane oxidation
49
50

51 Oxidation of cyclohexanol

52
53 In order to test the catalytic activity of complexes **1** - **3** towards the homogeneous MW-
54 assisted oxidation of cyclohexanol to cyclohexanone, the same operation conditions of the oxidation
55 of cyclohexane were applied (see experimental part) except that aq. *tert*-butyl hydroperoxide
56
57
58
59
60

(TBHP) was used as oxidizing agent, typically 1.5 h reaction time at 60 °C and in a solvent- and additive-free medium under MW radiation (Scheme 4).



Scheme 4 MW-assisted neat oxidation of cyclohexanol to cyclohexanone with *tert*-butyl hydroperoxide catalysed by **1–3**.

Under the adopted conditions, complexes **1** - **3** are able to catalyse the oxidation of cyclohexanol leading to yields of cyclohexanone in the range of 36 - 79% (Table 4, entries 1, 3 and 5). However, by performing the reactions at higher temperatures, considerably higher yields of cyclohexanone (up to 94% for **3** at 100 °C, entry 8, Table 4) are achieved in shorter reaction times (0.5 h, Table 4). Decomposition of H₂O₂ hampered its use at temperatures higher than 60 °C and therefore it was replaced by TBHP. The optimal reaction temperature for catalysts **1** - **3** was found to be 100 °C (see Fig. 4). A high selectivity towards the formation of the ketone (>99%) was displayed by these MW-assisted reactions, since only the unreacted alcohol (apart from cyclohexanone) was detected by GC–MS analysis of the final reaction mixtures.

Table 4. MW-assisted solvent-free oxidation of cyclohexanol using **1** - **3** as catalysts.^a

Entry	Catalyst	Reaction time /h	Temperature /°C	Yield ^b /%	TOF /h ⁻¹ ^c
1	1	1.5	60	36	120
2		0.5	100	61	
3	2	1.5	60	73	243
4		0.5	100	87	870
5		1.5	60	79	263
8	3	0.5	100	94	940
9 ^d		0.5	100	6	60
10 ^e	-	0.5	100	2	20
11	VO ₂ SO ₄	0.5	100	20	100
12	[VO(acac) ₂]	0.5	100	37	185

^aReaction conditions unless stated otherwise: 2.5 mmol of cyclohexanol, 5.0 μmol (0.2 mol% vs. substrate) of **1** - **3**, 5.0 mmol of TBHP (70% in H₂O) under MW radiation. ^bMoles of cyclohexanone per 100 moles of cyclohexanol. ^cTOF = number of moles of cyclohexanone per mol of catalyst (TON) per hour. ^dIn the presence of NHP₂. ^eWithout catalyst.

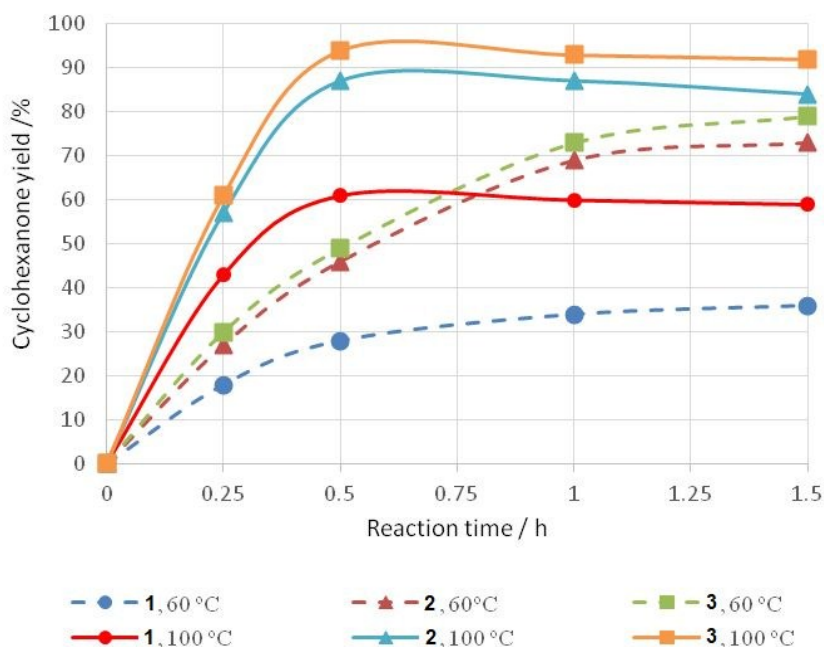


Fig. 4 Influence of the temperature and time on the yield of cyclohexanone obtained by MW-assisted oxidation of cyclohexanol with TBHP.

The present catalytic system displays a high activity. For example, it allows the fast (30 min.) almost quantitative formation of cyclohexanone (Fig. 4). Aerobic (by O₂) conversions (up to 90%) of cyclohexanol to cyclohexanone were previously obtained in the presence of N-hydroxyphthalimide as a radical producing agent and the co-catalyst [VO(acac)₂],⁵⁶ although requiring at least 18 h reaction time.

The peroxidative oxidation of cyclohexanol is believed to proceed mainly via a radical mechanism which involves both carbon- and oxygen-centred radicals,⁵⁷⁻⁵⁹ in view of the strong inhibition effect observed when it is carried out in the presence of an oxygen-radical trap such as Ph₂NH (Table 4, entry 9). It may involve *e.g.*, ^tBuO[•] and ^tBuOO[•] radicals produced in the V promoted decomposition of TBHP^{60,61} according to the equations 10 – 15.





It may also proceed via the coordination of the alcohol substrate to an active site of the catalyst, and its deprotonation to form the alkoxide ligand, followed by a metal-centred dehydrogenation.⁶²⁻⁶⁴

Theoretical calculations

Aiming to elucidate the plausible mechanism of the alkane oxidation with peroxides catalysed by complexes **1-3**, quantum chemical (DFT) calculations have been carried out. In accord with the experimental data (see above) and previous experimental and theoretical studies of the related V catalytic systems,⁵¹⁻⁵³ the global mechanism is of a radical type involving the formation of the radical species RO[•] (or HO[•] if H₂O₂ is used as an oxidant). This radical then oxidises the alkane molecule R-H abstracting a hydrogen atom to give the corresponding alkyl radical R[•]. The latter species reacts with molecular oxygen yielding finally alkyl hydroperoxide ROOH detected experimentally. The rate limiting step of the whole process is the generation of the RO[•] (HO[•]) radical.

The first mechanistic proposal for the formation of HO[•] radicals from H₂O₂ was formulated by Haber and Weiss⁶⁵ for the Fenton system (Fe(II) + H₂O₂).⁶⁶ In this mechanism, HO[•] radicals are directly formed upon the homolytic HO-OH bond cleavage in the hydrogen peroxide molecule. As a result, one of the generated HO[•] radicals is reduced by Fe(II) to the OH⁻ anion, and complex [Fe^{III}(H₂O)₅(OH)]²⁺ is formed (reaction 16). At the second step, another H₂O₂ molecule reacts with the Fe(III) hydroxo complex regenerating the initial catalyst and producing the HOO[•] radical (reaction 17).



For the catalytic systems with the metal in its highest oxidation state [*e.g.*, V(V) or Re(VII)], a modified mechanistic scheme was proposed.^{51-53,67,68} In this case, the sequence of the main reaction steps is inverted, *i.e.*, firstly, reduction of the metal centre in the catalyst by a peroxide (H₂O₂, ROOH) occurs (reaction 18, *n* is the oxidation state of the metal) and then the second peroxide molecule oxidizes the {M^{(*n*-1)}}H intermediate generating the HO[•] (RO[•]) radical (reaction

At the next step, a proton migration from the coordinated H_2O_2 to the methoxy ligand occurs via transition state **TS1** to give complex $[\text{V}^{\text{V}}(=\text{O})(\text{L})(\text{OOH})(\text{MeOH})]$ (**5**) with the activation barrier of 16.0 kcal/mol. Transition state **TS1** has a 6-membered cyclic structure of the reaction centre and it includes one H_2O molecule which plays the role of the proton shuttle. It was found^{51-53,67,68} that such a water assisted proton transfer is more favorable than the direct H^+ shift via a four-membered cyclic TS without involvement of any proton shuttle. The proton transfer from H_2O_2 to the ligand L or to the oxo-ligand is less favorable.

Complex **5** can lose the HOO^\bullet radical to give intermediate $[\text{V}^{\text{IV}}(=\text{O})(\text{L})(\text{MeOH})]$ **6**. This process corresponds to the reduction of V(V) to V(IV) by H_2O_2 and it is significantly endoergic (by 12.0 kcal/mol). Following addition of a second H_2O_2 molecule to **6** gives complex $[\text{V}^{\text{IV}}(=\text{O})(\text{L})(\text{H}_2\text{O}_2)(\text{MeOH})]$ (**7**). Then, reaction can follow two possible pathways. The first one includes the elimination of the methanol molecule in **7** to give $[\text{V}^{\text{IV}}(=\text{O})(\text{L})(\text{H}_2\text{O}_2)]$ (**8**) followed by the water assisted proton transfer from H_2O_2 to the oxo ligand leading to complex $[\text{V}^{\text{IV}}(\text{L})(\text{OH})(\text{OOH})]$ (**9**) via **TS2**. Finally, the O–OH bond cleavage upon reduction by V(IV) with generation of HO^\bullet can occur in **9** via **TS3** with rather low activation barrier ($\Delta G_s^\ddagger = 10.1$ kcal/mol).

Another pathway includes two consecutive proton transfers in **7** from H_2O_2 to the ligand L and then to the oxo-ligand to give finally complex $[\text{V}^{\text{IV}}(\text{L})(\text{OH})(\text{OOH})(\text{MeOH})]$ (**12**). The formation of the HO^\bullet radical occurs upon the O–OH bond cleavage in **12** upon reduction by V(IV) via **TS6** ($\Delta G_s^\ddagger = 9.1$ kcal/mol) with the simultaneous extrusion of the methanol molecule. The first pathway ($7 - \text{MeOH} \rightarrow 8 \rightarrow 9 \rightarrow 10 + \text{HO}^\bullet$) is significantly (by 15.8 kcal/mol) more favorable than the second one ($7 \rightarrow 11 \rightarrow 12 \rightarrow 10 + \text{HO}^\bullet + \text{MeOH}$).

The rate limiting transition state of the whole process of the HO^\bullet generation for this mechanism is **TS3**. The overall activation barrier is 38.2 kcal/mol. This value seems to be too high to permit the efficient realization of the reaction even under MW conditions. Thus, the mechanism of the radical formation from peroxides usually accepted for the V(V) catalysts does not seem to be feasible for the particular catalyst **1**.

Mechanism based on the simple coordination of H_2O_2 (Mechanism II). Meanwhile, the calculations indicated that the energy of the homolytic O–O bond cleavage in complex **4** is surprisingly low being only 22.3 kcal/mol (compared with the 47.5 kcal/mol in free H_2O_2). Hence, a simple coordination of H_2O_2 to the metal centre of the catalyst activates the peroxide towards the HO^\bullet radical generation by 25.2 kcal/mol. The reason of such a tremendous activation of H_2O_2 becomes clear from the analysis of the electronic structure of complex $[\text{V}(=\text{O})(\text{L})(\text{OMe})(\text{OH})]$ (**13**)

– the product of the O–O bond cleavage in **4**. As shown in Fig. 5, the spin electron density in **13** is delocalized among the atoms of the ligand L. Therefore, as a result of the O–O bond rupture in **4**, the HO• ligand bound to V is reduced to OH⁻ by the ligand L which is oxidized to L^{•+}. At the same time, the *oxidation state of vanadium is not changed* remaining to be +V. Such an intramolecular redox process significantly stabilizes one of the O–O bond cleavage products accounting for the significant decrease of the O–O bond dissociation energy. It is important to mention that the ligand L in complex **4** being redox active plays the same role as a transition metal does in the classical Fenton or Fenton-like mechanisms, *i.e.* it reduces one of the HO• radicals to OH⁻.

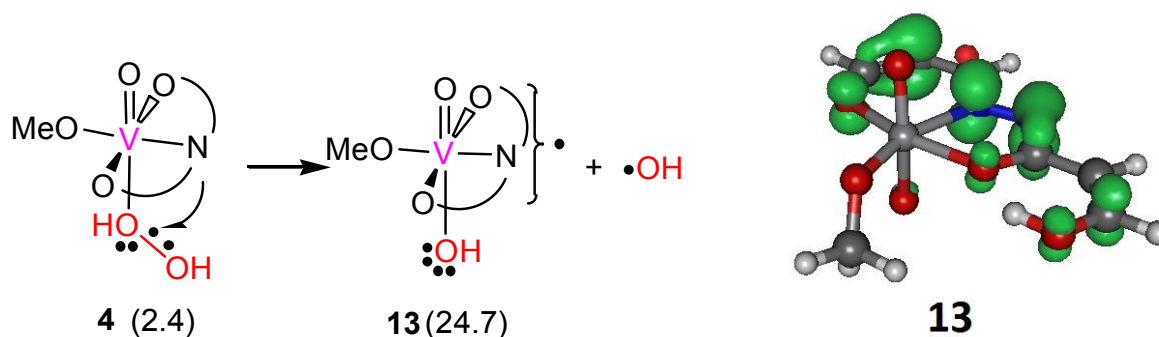
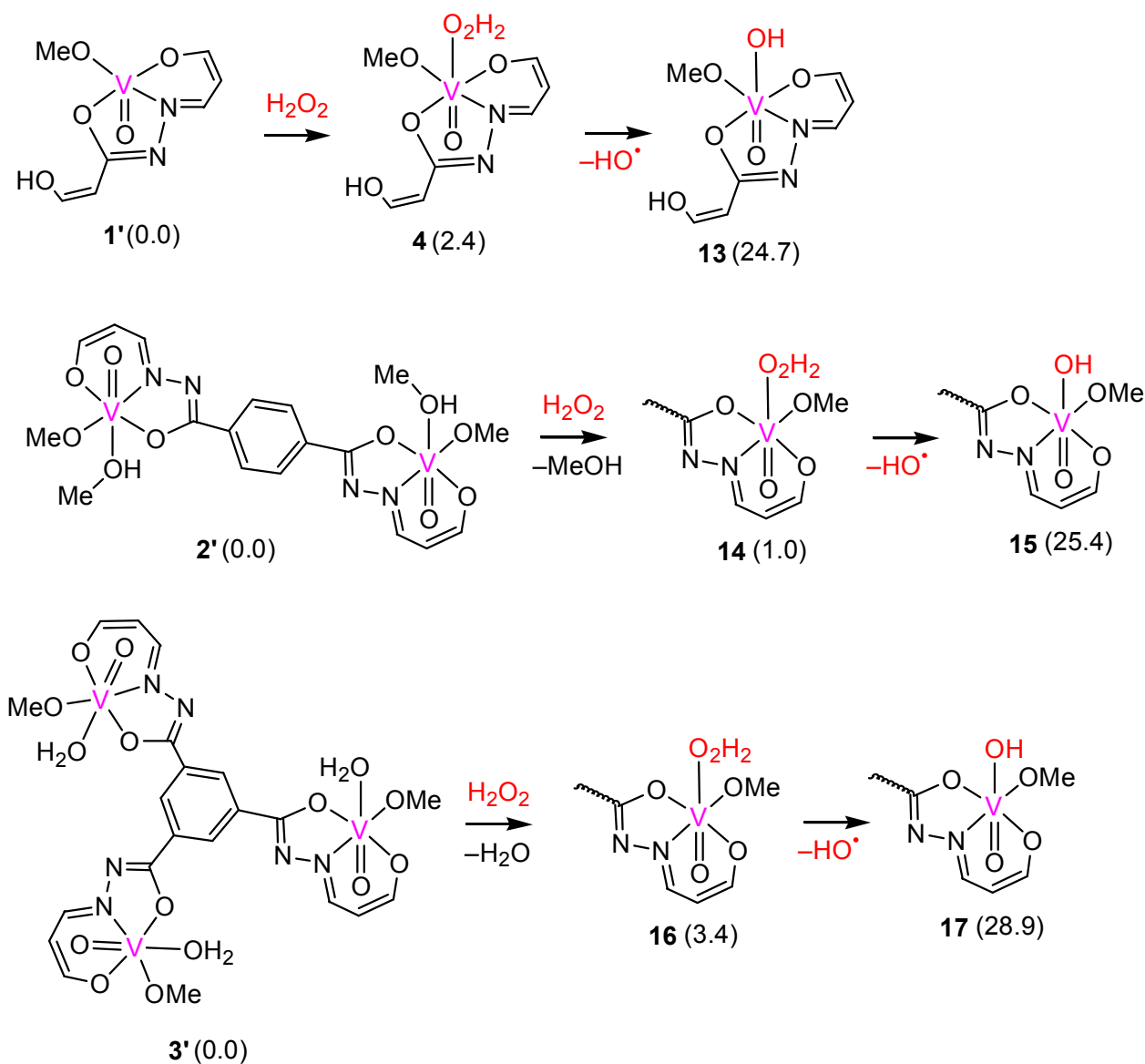


Fig. 5 The HO–OH bond cleavage and intramolecular electron transfer in complex **4** and spin density distribution in **13**. The ΔG_s values are indicated in kcal/mol relative to **1**'.

The O–O bond cleavage energy in the hydrogen peroxide complexes is slightly higher for the model bi and trinuclear catalysts **2**' and **3**' compared to **1**' (22.3, 24.4 and 25.5 kcal/mol for **1**', **2**' and **3**', respectively, Scheme 7). This qualitatively correlates with the experimental data revealing the lower product yields per metal unit for the catalysts **2** and **3** (Table 1).

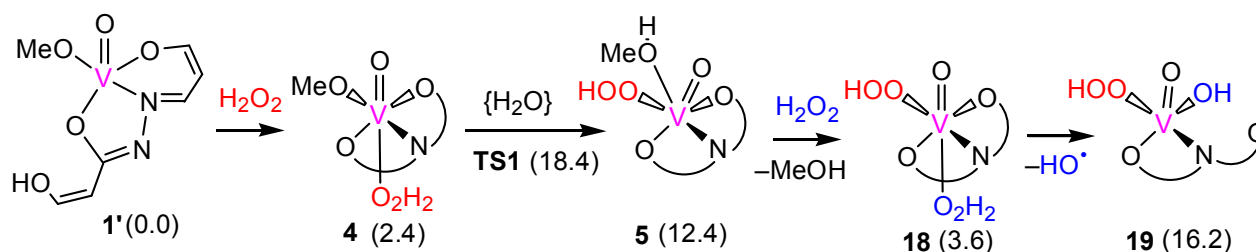


Scheme 6. Mechanism based on the simple coordination of H_2O_2 (Mechanism II) for the model catalysts **1'**–**3'**. The ΔG_s values are indicated in kcal/mol relative to initial catalyst.

Mechanism II involving two H_2O_2 molecules. In the previous works, some of us demonstrated that two H_2O_2 molecules participate in the HO^\bullet radical generation catalyzed by the aqua complexes $[\text{M}(\text{H}_2\text{O})_n]^{p+}$ ($\text{M} = \text{Al}, \text{Ga}, \text{In}, \text{Sc}, \text{Y}, \text{La}, \text{Be}, \text{Zn}, \text{Cd}, \text{Bi}$).⁶⁹⁻⁷¹ In this mechanism, one H_2O_2 molecule is a direct source of HO^\bullet whereas another H_2O_2 molecule is a precursor of the redox active OOH^- ligand. The possibility of a similar mechanism for the V catalysts under study was also analyzed.

This mechanism includes the coordination of H_2O_2 to **1'**, proton migration to the methoxy ligand (these two steps were discussed above), liberation of the methanol and coordination of the

second H₂O₂ molecules to give complex [V^V(=O)(L)(OOH)(H₂O₂)] (**18**) (Scheme 7). The HO–OH bond cleavage in **18** affords the HO• radical and complex [V(=O)(L)(OOH)(OH)] (**19**). The hydrogen peroxide molecule in **18** is even more activated than that in **4**, the HO–OH bond cleavage energy being only 12.6 kcal/mol. The spin density in **19** is also delocalized along the ligand L (Fig. 6). Thus, the joint presence of both L and OOH⁻ ligands in the complex molecule activates H₂O₂ most efficiently despite the OOH⁻ ligand is not redox active in this case. The reduction of the ligated H₂O₂ (with O–O bond cleavage) to HO• and hydroxide ligand is carried out by the L²⁻ ligand (to form L⁻) with preservation of the metal oxidation state (V) and of the OOH⁻ ligand. A related type of behaviour was suggested by some of us for a carbohydrazone ligand (on the basis of electrochemical studies)⁷² and for a quinolin-8-ate ligand.⁷³



Scheme 7. Mechanism II involving two H₂O₂ molecules. The ΔG_s values are indicated in kcal/mol relative to **1'**.

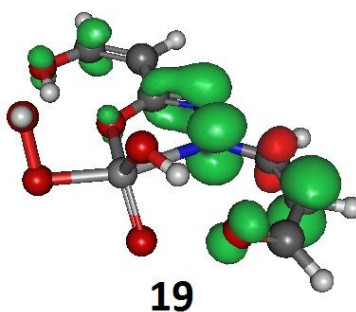


Fig. 6 Spin density distribution in **19**.

Due to the change of the system spin state as a result of the HO–OH bond cleavage in **18**, the straightforward estimate of the activation energy for this step is not a simple task. Therefore, the relaxed scan of the triplet and singlet potential energy surfaces (PESs) for the HO–OH bond cleavage in **18** was carried out (Fig. 7). On one hand, the increase of the HO–OH bond distance in **18** at the singlet close shell PES (which corresponds to the heterolytic HO–OH bond rupture) results in the monotonous enhancement of the system energy until the HO–OH distance of 2.12 Å. On the

other hand, the excitation of **18** to the triplet spin state requires only 12.1 kcal/mol. The scan energy curve for the triplet PES has a maximum at the HO–OH distance of 1.82 Å. Curves of both close shell and triplet energy scans intersect at $d(\text{HO–OH}) \approx 1.92$ Å. A singlet biradical structure **20** was optimized using the broken symmetry approach starting from the intersection point with the fixed HO–OH distance and all other internal coordinates being relaxed. The energy of **20** determines the highest limit of the activation energy. The thus estimated activation energy limit of the homolytic HO–OH bond cleavage in **18** is 29.5 kcal/mol and the overall activation energy limit for the whole reaction of the HO• generation (*i.e.* that relative to the level of initial reactants) is 33.1 kcal/mol (both values are in terms of Gibbs free energy in solution). The last value is rather high indicating that under thermal conditions the catalytic activity of the V complexes under study should be rather low. However, under the MW conditions, the reaction should be efficient due to strong and rapid local overheating, pressure enhancement and possible nonthermal effects on the preexponential factor in the Arrhenius equation. All this correlates with the experimental observations demonstrating a crucial role of MW in the reaction.

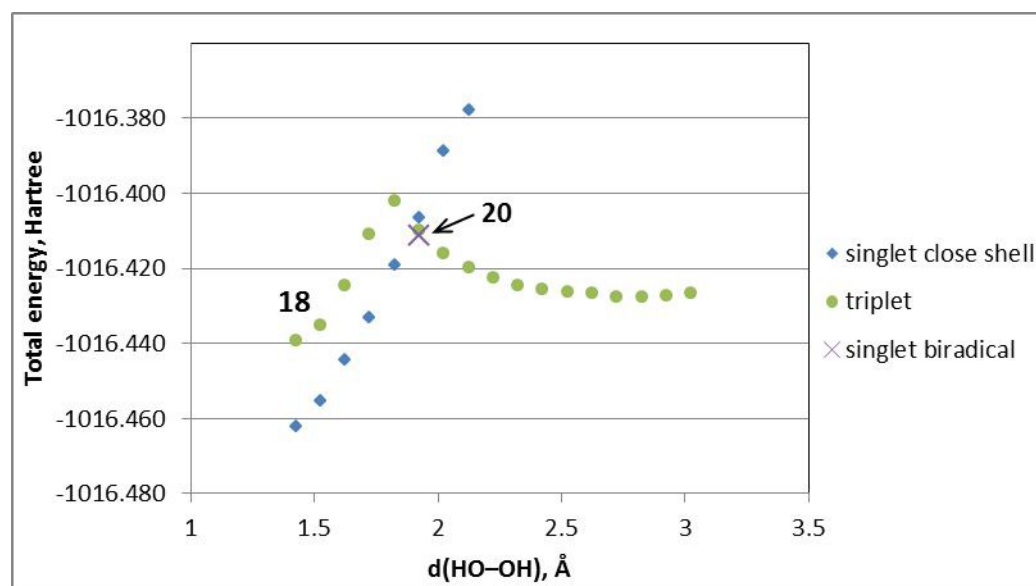


Fig. 7 Energy scan for the HO–OH bond cleavage in **18**. The HO–OH distance was fixed while all other internal coordinates were relaxed.

Experimental

General Materials and Procedures

All synthetic work was performed in air. The reagents and solvents were obtained from commercial sources and used as received, *i.e.*, without further purification or drying. [VO(OEt)(L¹)] (**1**)^{38,39} and [{VO(OEt)(EtOH)}₂(L²)] (**2**)²⁸ were synthesized as reported. VOSO₄·3H₂O was used as the metal source for the synthesis of complex **3**. C, H, and N elemental analyses were carried out by the Microanalytical Service of the Instituto Superior Técnico. Infrared spectra (4000–400 cm⁻¹) were recorded on a BRUKER VERTEX 70 or Jasco FT/IR-430 instrument in KBr pellets, wavenumbers are in cm⁻¹. Mass spectra were run in a Varian 500-MS LC Ion Trap Mass Spectrometer equipped with an electrospray (ESI) ion source. For electrospray ionization, the drying gas and flow rate were optimized according to the particular sample with 35 p.s.i. nebulizer pressure. Scanning was performed from *m/z* 100 to 1200 in acetonitrile solution. The compounds were observed in the positive mode (capillary voltage = 80–105 V). The ¹H NMR spectra were recorded at room temperature on a Bruker Avance II + 300 (UltraShield™ Magnet) spectrometer operating at 300.130 MHz. The chemical shifts are reported in ppm using tetramethylsilane as the internal reference. ⁵¹V NMR spectra were recorded on a Bruker 400 UltraShield spectrometer at ambient temperature (297 K) in DMSO-*d*₆. The vanadium chemical shifts were quoted relative to external [VOCl₃]. The catalytic investigations under microwave irradiation were performed in a focused Anton Paar Monowave 300 microwave reactor. The UV-vis absorption spectra in the 200 – 700 nm region were recorded with a scan rate of 240 nm·min⁻¹ by using a Lambda 35 UV-vis spectrophotometer (Perkin-Elmer) in 1.00 cm quartz cells at room temperature, with a concentration of **1-3** of 1.0 × 10⁻⁶ mol L⁻¹ in CH₃CN and under catalytic conditions.

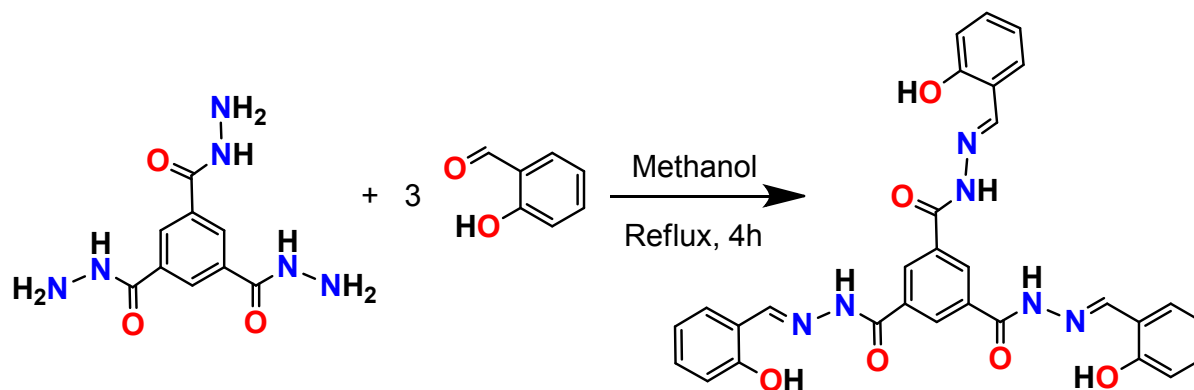
Synthetic procedures

Synthesis of H₆L³

The Schiff base pro-ligand tris(2-hydroxybenzylidene)benzene-1,3,5-tricarbohydrazide (H₆L³) was prepared by a reported method³⁸ upon condensation of benzene-1,3,5-tricarbohydrazide with 3 equivalents of 2-hydroxybenzaldehyde in methanol (Scheme 1).

H₆L³: Yield 86%. Anal. Calcd for C₃₀H₂₄N₆O₆ (H₆L³): C, 63.82; H, 4.28; N, 14.89. Found: C, 63.76; H, 4.26; N, 14.84. IR (KBr; cm⁻¹): 3423 ν(OH). 1607 ν(C=N), 1253 ν(C–O) enolic and 1071 ν(N–N). ¹H NMR (DMSO-*d*₆, δ): 12.44 (s, 1H, OH), 11.17 (s, 1H, OH), 9.01 (s, 1H, OH), 8.73 (s,

3H, -CH=N), 7.63-6.92 (m, 15H, C₆H₄). IR (KBr; cm⁻¹): 3328 ν(OH), 2957 ν(NH), 1658 ν(C=O), 1590 ν(C=N).



Scheme 8 Synthesis of H₆L³.

Synthesis of [*VO(OMe)(H₂O)*]₃(L³).2H₂O (**3**)

To 30 mL of methanol solution of H₆L (0.565 g, 1.00 mmol), 0.651 g (3.00 mmol) of VOSO₄·3H₂O was added and the reaction mixture was refluxed for 2 h in an oil bath, in open air. The resultant reddish-brown solution was filtered, and the filtrate was kept in air. After 3 d, single crystals of **3** (Scheme 1, Fig. 1) were isolated, washed 3 times with cold methanol and dried in open air.

Yield 67%. Anal. Calcd for C₃₃H₃₇N₆O₁₇V₃: C, 42.05; H, 3.96; N, 8.92. Found: C, 42.01; H, 3.92; N, 8.89. IR (KBr; cm⁻¹): 4218 ν(O-H), 4061ν(O-H), 1602 ν(C=N), 1250 ν(C-O) enolic, 1036 ν(N-N), 1007 ν(V=O), 986 ν(V=O) and 914 ν(V=O). ¹H NMR (DMSO-d₆, δ): 8.62 (s, 3H, -CH=N), 7.65-6.94 (m, 15H, C₆H₄) 3.74 (s, broad, 9H, -CH₃). ⁵¹V NMR (DMSO-d₆, δ): -529, -541 and -579. *m/z* 907 [(M-2H₂O)+H]⁺ (100 %).

X-ray measurements

X-ray single crystal of complex **3** was immersed in cryo-oil, mounted in Nylon loops and measured at room temperature of 298 K. Intensity data were collected using a Bruker APEX-II PHOTON 100 with graphite monochromated Mo-Kα (λ 0.71073) radiation. Data were collected using omega scans of 0.5° per frame and full sphere of data were obtained. Cell parameters were

retrieved using Bruker SMART⁷⁴ software and refined using Bruker SAINT⁷⁴ on all the observed reflections. Absorption corrections were applied using SADABS.⁷⁴ Structures were solved by direct methods by using SIR97⁷⁵ and refined with SHELXL–2018/1.⁷⁶ Calculations were performed using the WinGX System–Version 2014.1.⁷⁷ Least square refinements with anisotropic thermal motion parameters for all the non-hydrogen atoms and isotropic for the remaining atoms were employed. All hydrogen atoms bonded to carbon were included in the model at geometrically calculated positions and refined using a riding model. $U_{\text{iso}}(\text{H})$ were defined as $1.2U_{\text{eq}}$ of the parent carbon atoms for phenyl and benzylic residues and $1.5U_{\text{eq}}$ of the parent carbon atoms for the methyl groups. The hydrogen atoms of the free and coordinated water molecules have been inserted in calculated positions obtained with CALC-OH routine; the isotropic thermal parameter was set at 1.5 times the average thermal parameter of the belonging oxygen atoms and refined with DFIX and DANG restraints. The structure contains residual electron density (12 electrons) in a void of 61.7 \AA^3 which was removed by means of PLATON SQUEEZE routine.⁷⁸ CCDC 1880765 contains the supplementary crystallographic data for **3**. These data can be obtained free of charge from The Cambridge Crystallographic Data Centre via www.ccdc.cam.ac.uk/data_request/cif.

Solvent-free microwave-assisted catalytic oxidation of cyclohexane and cyclohexanol

The catalytic oxidations of cyclohexane or cyclohexanol were carried out in sealed cylindrical Pyrex tubes (10 mL capacity reaction tube with a 13 mm internal diameter), under focused microwave irradiation (MW) in an Anton Paar Monowave 300 reactor fitted with a rotational system and an IR temperature detector.

Gas chromatographic (GC) measurements were carried out using a FISIONS Instruments GC 8000 series gas chromatograph equipped with a FID detector and a capillary column (DB-WAX, column length: 30 m; column internal diameter: 0.32 mm) and run by the software Jasco-Borwin v.1.50. The temperature of injection was 240 °C. After the injection, the reaction temperature was maintained at either 100 °C (oxidation of cyclohexane) or 140 °C (oxidation of cyclohexanol) for 1 min, then raised, by 10 °C/min, either to 160 °C (oxidation of cyclohexane) or 220 °C (oxidation of cyclohexanol) and held at this temperature for 1 min. Helium was used as the carrier gas.

GC-MS analyses were performed using a Perkin Elmer Clarus 600 C instrument (He as the carrier gas). The ionization voltage was 70 eV. Gas chromatography was conducted in the temperature-programming mode, using a SGE BPX5 column (30 m × 0.25 mm × 0.25 μm).

Typical procedures for the catalytic oxidation of cyclohexane or cyclohexanol and products analysis

Typical reaction conditions are as follows: catalyst **1 - 3** (1-10 μmol , 0.04 - 0.4 mol% vs. substrate) was added to 2.50 mmol of substrate, whereafter 5.00 mmol of 30% aqueous hydrogen peroxide (oxidation of cyclohexane) or 70% aqueous *tert*-butyl hydroperoxide (TBHP, oxidation of cyclohexanol) were introduced in the tube. For the assays in the presence of a radical trap, NHPH₂ in stoichiometric amount relative to the oxidant was added. The tube was placed in the microwave (MW) reactor and the mixture stirred (800 rpm) and irradiated (10 - 25 W) for 0.25 – 3 h at 60 °C (oxidation of cyclohexane) or 100 °C (oxidation of cyclohexanol). After the reaction, the mixture was allowed to cool down to room temperature.

Solution samples were analysed by GC (internal standard method) after addition of nitromethane (as the standard compound). Reaction products were identified by comparison of their retention times with those from known reference compounds, and by comparing their mass spectra to fragmentation patterns obtained from the NIST spectral library stored in the computer software of the mass spectrometer.

In the case of the oxidation of cyclohexane, the product yields were obtained after the reduction of the reaction sample with an excess of triphenylphosphine, following a method developed by Shul'pin.⁴⁶⁻⁴⁸ CyOOH was then reduced to cyclohexanol, with formation of O=PPh₃ as a by-product.

Blank experiments, in the absence of any catalyst, were performed under the studied reaction conditions. No considerable conversion of cyclohexane was observed and only traces (< 0.5%) of cyclohexanone were generated in the V-free systems.

Computational Details

The full geometry optimization of all structures and transition states (TSs) has been carried out at the DFT level of theory by using the M06 functional⁷⁹ with the help of the Gaussian 09 program package.⁸⁰ No symmetry operations were applied. The geometry optimization was carried out by using a relativistic Stuttgart pseudopotential which describes 10 core electron (MDF10) and the appropriate contracted basis set (8s7p6d1f)/[6s5p3d1f]⁸¹ for the vanadium atoms and the 6-31G* basis set for other atoms. Single-point calculations were performed on the basis of the equilibrium geometries found by using the 6-311+G** basis set for non-metal atoms.

The Hessian matrix was calculated analytically for the optimized structures to prove the location of correct minima (no imaginary frequencies) or saddle points (only one imaginary frequency) and to estimate the thermodynamic parameters, with the latter calculated at 25 °C. The nature of all transition states was investigated by analysis of the vectors associated with the imaginary frequency and by the calculations of the intrinsic reaction coordinates (IRC) by using the method developed by Gonzalez and Schlegel.⁸²⁻⁸⁴

The total energies corrected for solvent effects E_s were estimated at the single-point calculations on the basis of gas-phase geometries at the CPCM-M06/6-311+G**//gas-M06/6-31G* level of theory using the polarizable continuum model in the CPCM version^{85,86} with cyclohexane as solvent. The UAKS model was applied for the molecular cavity, and dispersion, cavitation and repulsion terms were taken into account. The entropic term in cyclohexane solution (S_s) was calculated according to the procedure described by Wertz⁸⁷ and Cooper and Ziegler⁸⁸ using eqn. 20–23:

$$\Delta S_1 = R \ln(V_{m,liq}^s/V_{m,gas}) \quad (20)$$

$$\Delta S_2 = R \ln(V_m^o/V_{m,liq}^s) \quad (21)$$

$$\alpha = [S^{o,s}_{liq} - (S^{o,s}_{gas} + \Delta S_1)]/[S^{o,s}_{gas} + \Delta S_1] \quad (22)$$

$$S_s = S_g + \Delta S_{sol} = S_g + [\Delta S_1 + \alpha(S_g + \Delta S_1) + \Delta S_2] = S_g + [(-10.77 \text{ cal/mol}\cdot\text{K}) - 0.19(S_g - 10.77 \text{ cal/mol}\cdot\text{K}) + 4.42 \text{ cal/mol}\cdot\text{K}] \quad (23)$$

where S_g is the gas-phase entropy of solute, ΔS_{sol} is the solvation entropy, $S^{o,s}_{liq}$, $S^{o,s}_{gas}$ and $V_{m,liq}^s$ are the standard entropies and molar volume of the solvent in the liquid or gas phases (204.35 and 298.19 J/mol·K and 107.83 mL/mol, respectively, for cyclohexane), $V_{m,gas}$ is the molar volume of the ideal gas at 25 °C (24450 mL/mol), V_m^o is the molar volume of the solution that correspond to the standard conditions (1000 mL/mol). The enthalpies and Gibbs free energies in solution (H_s and G_s , respectively) were estimated using the expressions 24 and 25

$$H_s = E_s(6-311+G^{**}) + H_g(6-31G^*) - E_g(6-311+G^{**}) \quad (24)$$

$$G_s = H_s - TS_s \quad (25)$$

where E_s and E_g are the total energies in solution and the gas phase and H_g is the gas-phase enthalpy calculated at the corresponding level. Gibbs free energies in solution are discussed in this work if not stated otherwise.

Conclusions

In this study, we have successfully investigated and compared the catalytic activity of three oxidovanadium(V) complexes (**1-3**) with azine based aroylhydrazone ligands having a similar type of tridentate ONO chelate pockets, differing in their nuclearities, *i.e.*, mononuclear (**1**), binuclear (**2**) and trinuclear (**3**), towards MW-assisted homogeneous oxidation of cyclohexane and a secondary alcohol (cyclohexanol). They act as homogeneous catalysts for the MW-assisted and solvent-free (with aq. TBHP) oxidation of cyclohexane and cyclohexanol, via radical mechanisms, affording the oxygenate products in high selectivity. Complex **1** exhibited the highest catalytic activity per V centre (in terms of yield and TON values) for both alkane and alcohol oxidations. However, complex **3** led to an almost quantitative conversion of cyclohexanol into cyclohexanone. Considering the overall catalytic activity per mole of catalyst, the following order was observed: **3**>**2**>**1**.

Other advantages of the present catalytic systems are the mild and environmentally benign conditions concerning (i) a solvent- and additive-free protocol, (ii) the use of environmentally acceptable oxidant (aq. TBHP) and energy source (MW irradiation), and (iii) a very short reaction time. These are significant features towards the development of a sustainable chemical process for both oxidations.

A mechanism of the HO• radical generation – the rate limiting step of the cyclohexane oxidation by H₂O₂ – was investigated in detail using theoretical DFT methods. This mechanism is different from those usually accepted for the Fenton or Fenton-like systems and it includes (i) coordination of H₂O₂ to the catalyst molecule, (ii) proton transfer from ligated H₂O₂ to the methoxy ligand and elimination of the formed methanol molecule and (iii) coordination of a second H₂O₂ molecule followed by HO–OH bond cleavage to give HO• (Scheme 7). The activation of the ligated H₂O₂ in complex **18** towards O–O bond cleavage is associated with the redox active nature of the ligand L in the catalyst molecule, whereby this azine based ligand (instead of the metal or of HOO⁻ ligand) acts as the reducing agent of the H₂O₂ ligand to cleave its O–O bond.

This study demonstrates the non-innocent character of this type of azine based aroylhydrazone ligand, which provides a key role in the peroxide O–O bond cleavage in the

peroxidative alkane oxidation. It also concerns the perspective of varying the vanadium nuclearity in catalysts for such oxidation reactions. These issues deserve to be further explored and can open up a new window to the vanadium chemistry.

Conflicts of interest

There are no conflicts of interest to declare.

Acknowledgment

Authors are grateful to the Fundação para a Ciência e a Tecnologia (FCT, projects UID/QUI/00100/2013, PTDC/QEQ-ERQ/1648/2014 and PTDC/QEQ-QIN/3967/2014), Portugal, for financial support. M.S. acknowledges the FCT for a working contract "DL/57/2017" (NT 13/CQE). Authors are thankful to the Portuguese NMR Network (IST-UL Centre) for access to the NMR facility and the IST Node of the Portuguese Network of mass-spectrometry for the ESI-MS measurements.

Supporting information

Supplementary **Tables TS1-TS6**. CCDC 1880765 for **3** contains the supplementary crystallographic data for this paper. These data can be obtained free of charge from The Cambridge Crystallographic Data Centre via www.ccdc.cam.ac.uk/data_request/cif. Supplementary data to this article can be found online at

References

- 1 M. Sutradhar, L. M. D. R. S. Martins, M. F. C. Guedes da Silva and A. J. L. Pombeiro, *Coord. Chem. Rev.*, 2015, **301-302**, 200-239.
- 2 J. A. L. da Silva, J. J. R. Frausto da Silva and A. J. L. Pombeiro, *Coord. Chem. Rev.*, 2011, **255**, 2232- 2248.
- 3 V. Conte, A. Coletti, B. Floris, G. Licini and C. Zonta, *Coord. Chem. Rev.*, 2011, **255**, 2165-2177.
- 4 M. Sutradhar and A. J. L. Pombeiro, *Cord. Chem. Rev.*, 2014, **265**, 89-124.
- 5 A. G. J. Ligtenbarg, R. Hage and B. L. Feringa, *Coord. Chem. Rev.*, 2003, **237**, 89–101.
- 6 A.E. Shilov, G.B. Shul'pin, *Chem. Rev.* 97 (1997) 2879–2932.
- 7 M. Sutradhar and A. J. L. Pombeiro, *Vanadium Complexes in Catalytic Oxidations*, in J. Reedijk, (Ed.) Elsevier Reference Module in Chemistry, Molecular Sciences and Chemical Engineering. Waltham, MA: Elsevier (2017). doi.org/10.1016/B978-0-12-409547-2.13525-5.

- 1
2 8 G. B. Shul'pin, *Catalysts*, 2016, **6**, 50(1-40).
3 9 A. M. Kirilov and G. B. Shul'pin, *Coord. Chem. Rev.*, 2013, **257**, 732-754.
4 10 G. B. Shul'pin, *Org. Biomol. Chem.*, 2010, **8**, 4217-4228.
5 11 A. J. L. Pombeiro, in *Advances in Organometallic Chemistry and Catalysis*, ed: A. J. L.
6 Pombeiro, John Wiley & Sons: Hoboken, NJ, USA, 2014, Ch. 2, pp. 15–25.
7 12 A. E. Shilov and G. B. Shul'pin, *Activation and Catalytic Reactions of Saturated Hydrocarbons*
8 *in the Presence of Metal Complexes*, Kluwer Academic Publishers, Dordrecht, 2000.
9 13 J.-E. Backvall, *Modern Oxidation Methods*, Wiley-VCH, Weinheim, 2004.
10 14 A. J. L. Pombeiro (ed.), *Advances in Organometallic Chemistry and Catalysis*, John Wiley &
11 Sons: Hoboken, NJ, USA, 2014
12 15 G. B. Shul'pin, in *Transition Metals for Organic Synthesis*, ed.: M. Beller, C. Bolm, Vol. 2, 2nd
13 edn, Wiley-VCR, New York, 2004, Vol. 2, Ch. 2 p. 215.
14 16 A. E. Shilov and G. B. Shul'pin, *Chem. Rev.*, 1997, **97**, 2879-2932.
15 17 G. B. Shul'pin, *Mini-Rev. Org. Chem.*, 2009, **6**, 95-104.
16 18 R. H. Crabtree, *J. Chem. Soc., Dalton Trans.*, 2001, 2437-2450.
17 19 R. H. Liu, X. M. Liang, C. Y. Dong and X. Q. Hu, *J. Am. Chem. Soc.*, 2004, **126**, 4112-4113.
18 20 R. F. Nie, J. J. Shi, W. C. Du, W. S. Ning, Z. Y. Hou and F. S. Xiao, *J. Mater. Chem. A*, 2013, **1**,
19 9037-9045.
20 21 S. J. Liu, N. Zhang, Z. R. Tang and Y. J. Xu, *ACS Appl. Mater. Interfaces*, 2012, **4**, 6378-6385.
21 22 M. N. Kopylovich, A. P. C. Ribeiro, E. C. B. A. Alegria, N. M. R. Martins, L. M. D. R. S.
22 Martins and A. J. L. Pombeiro, *Adv. Organomet. Chem.*, 2015, **63**, 91-174.
23 23 Y. Y. Karabach, M. N. Kopylovich, K. T. Mahmudov and A. J. L. Pombeiro, in *Advances in*
24 *Organometallic Chemistry and Catalysis*, ed: A. J. L. Pombeiro, John Wiley & Sons: Hoboken, NJ,
25 USA, 2014, Ch. 18, pp. 233-245.
26 24 S. Horikoshi, N. Serpone, *Microwaves in Catalysis: Methodology and Applications*, John Wiley
27 & Sons, 2015.
28 25 M. Domarus, M. L. Kuznetsov, J. Marçalo, A. J. L. Pombeiro and J. A. L. da Silva, *Angew.*
29 *Chem. Int. Ed.*, 2016, **55**, 1489-1492.
30 26 D. Rehder, *Bioinorganic Vanadium Chemistry*, Wiley, Chichester, U. K., 2008.
31 27 G. B. Shul'pin and Y. N. Kozlov, *Org. Biomol. Chem.*, 2003, **1**, 2303–2306.
32 28 M. Sutradhar, N. V. Shvydkiy, M. F. C. Guedes da Silva, M. V. Kirillova, Y. N. Kozlov, A. J. L.
33 Pombeiro and G. B. Shul'pin, *Dalton Trans.*, 2013, **42**, 11791-11803.
34 29 M. Sutradhar, M. V. Kirillova, M. F. C. Guedes da Silva, L. M. D. R. S. Martins and A. J. L.
35 Pombeiro, *Inorg. Chem.*, 2012, **51**, 11229-11231.
36 30 M. Sutradhar, M. V. Kirillova, M. F. C. Guedes da Silva, C.-M. Liu and A. J. L. Pombeiro,
37 *Dalton Trans.*, 2013, **42**, 16578-16587.
38 31 M. Sutradhar, L. M. D. R. S. Martins, M. F. C. Guedes da Silva, E. C. B. A. Alegria, C.-M. Liu
39 and A. J. L. Pombeiro, *Dalton Trans.*, 2014, **43**, 3966-3977.
40 32 M. Sutradhar, L. M. D. R. S. Martins, S. A. C. Carabineiro, M. F. C. Guedes da Silva, J. G.
41 Buijnsters, J. L. Figueiredo and A. J. L. Pombeiro, *ChemCatChem.*, 2016, **8**, 2254-2266.
42 33 M. Sutradhar, L. M. D. R. S. Martins, M. F. C. Guedes da Silva and A. J. L. Pombeiro, *Appl.*
43 *Catal. A: Gen.*, 2015, **493**, 50-57.
44 34 M. Sutradhar, E. C. B. A. Alegria, T. Roy Barman, F. Scorcelletti, M. F. C. Guedes da Silva and
45 A. J. L. Pombeiro, *Mol. Catal.*, 2017, **439**, 224-232.
46 35 M. Sutradhar, L. M. D. R. S. Martins, M. F. C. Guedes da Silva, C.-M. Liu and A. J.
47 L. Pombeiro, *Eur. J. Inorg. Chem.*, 2015, 3959-3969.
48 36 M. Sutradhar, E. C. B. A. Alegria, M. F. C. Guedes da Silva, L. M. D. R. S. Martins and A. J. L.
49 Pombeiro, *Molecules*, 2016, **425**, 1-13.
50
51
52
53
54
55
56
57
58
59
60

- 1
2 37 M. Sutradhar, E. C. B. A. Alegria, K. T. Mahmudov, M. F. C. Guedes da Silva and A. J. L.
3 Pombeiro, *RSC Adv.*, 2016, **6**, 8079-8088.
4 38 M. Sutradhar, G. Mukherjee, M. G. B. Drew and S. Ghosh, *Inorg. Chem.*, 2006, **45**, 5150-5161.
5 39 R. Dinda, P. Sengupta, M. Sutradhar, T. C. W. Mak and S. Ghosh, *Inorg. Chem.*, 2008, **47**, 5634-
6 5640.
7 40 F. Jiang, O. P. Anderson, S. M. Miller, J. Chen, M. Mahroof-Tahir and D. C. Crans, *Inorg.*
8 *Chem.*, 1998, **37**, 5439-5451
9 41 M. R. Maurya, *Coord. Chem. Rev.*, 2019, **383**, 43-81.
10 42 D. C. Crans, K. A. Woll, K. Prusinskas, M. D. Johnson and E. Norkus, *Inorg. Chem.*, 2013, **52**,
11 12262-12275.
12 43 A. Levina, D. C. Crans and P. A. Lay, *Coord. Chem. Rev.*, 2017, **352**, 473-498.
13 44 C. C. McLauchlan, H. A. Murakami, C. A. Wallace and D. C. Crans, *J. Inorg. Biochem.*, 2018,
14 **186**, 267-279.
15 45 M. Sutradhar, T. Roy Barman, S. Ghosh and M. G. B. Drew, *J. Mol. Struct.* 2012, **1020**, 148-
16 152.
17 46 G. B. Shul'pin, *J. Mol. Catal. A: Chem.*, 2002, **189**, 39-66.
18 47 G. B. Shul'pin, *C. R. Chim.*, 2003, **6**, 163-178.
19 48 G. B. Shul'pin, Y. N. Kozlov, L. S. Shul'pina, A. R. Kudinov and D. Mandelli, *Inorg. Chem.*,
20 2009, **48**, 10480-10482.
21 49 Ullmann's Encyclopedia of Industrial Chemistry, 6th ed., Wiley-VCH, Weinheim, 2002.
22 50 D. E. Mears, A. D. Eastman, in *Kirk-Othmer Encyclopedia of Chemical Technology*, Vol. 13, 5th
23 ed. (Ed.: A. Seidel), Wiley, 2004, p. 706.
24 51 G. B. Shul'pin, Y. N. Kozlov, G. V. Nizova, G. Süß-Fink, S. Stanislas, A. Kitaygorodskiy and
25 V. S. Kulikova, *J. Chem. Soc. Perkin Trans.*, 2001, **2**, 1351-1371.
26 52 M. V. Kirillova, M. L. Kuznetsov, V. B. Romakh, L. S. Shul'pina, J. J. R. Fraústo da Silva, A. J.
27 L. Pombeiro and G. B. Shul'pin, *J. Catal.*, 2009, **267**, 140-157.
28 53 M. V. Kirilova, M. L. Kuznetsov, Y. N. Kozlov, L. S. Shul'pina, A. Kitaygorodskiy, A. J. L.
29 Pombeiro and G. B. Shul'pin, *ACS Catal.*, 2011, **1**, 1511-1520.
30 54 R. R. Fernandes, J. Lasri, M. F. C. Guedes da Silva, J. A. L. da Silva, J. J. R. Fraústo da Silva
31 and A. J. L. Pombeiro, *Appl. Catal. A: Gen*, 2011, **402**, 110-120.
32 55 G. Süß-Fink, L. Gonzalez and G. B. Shul'pin, *Appl. Catal., A: Gen*, 2001, **217**, 111-117.
33 56 P. J. Figiel, J. M. Sobczak and J. J. Ziółkowski, *Chem. Com.*, 2004, 244-245.
34 57 L. M. Slaughter, J. P. Collman, T. A. Eberspacher and J. I. Brauman, *Inorg. Chem.*, 2004, **43**,
35 5198-5204.
36 58 J. A. Howard, in *Free Radicals*, vol. II (J. K. Kochi, Ed.), Wiley, New York, 1973 p. 3.
37 59 J. M. Mattalia, B. Vacher, A. Samat and M. Chanon, *J. Am. Chem. Soc.*, 1992, **114**, 4111-4119.
38 60 L. Feldberg and Y. Sasson, *Tetrahedron Lett.* 1996, **37**, 2063-2066.
39 61 V. Mahdavi, M. Mardani, *J. Chem. Sci.*, 2012, **124**, 1107-1115.
40 62 M. V. N. de Souza, *Mini-Rev. Org. Chem.*, 2006, **3**, 155-165.
41 63 R. A. Sheldon and I. W. C. E. Arends, *Adv. Synth. Catal.*, 2004, **346**, 1051-1071.
42 64 P. J. Figiel, A. Sibaouih, J. U. Ahmad, M. Nieger, M. T. Räisänen, M. Leskelä and T. Repo, *Adv.*
43 *Synth. Catal.*, 2009, **351**, 2625-2632.
44 65 F. Haber and J. Weiss, *Naturwiss.*, 1932, **20**, 948-950.
45 66 H. J. H. Fenton, *J. Chem. Soc., Trans.*, 1894, **65**, 899-910.
46 67 R. Z. Khaliullin, A. T. Bell and M. Head-Gordon, *J. Phys. Chem. B*, 2005, **109**, 17984-17992.
47 68 M. L. Kuznetsov and A. J. L. Pombeiro, *Inorg. Chem.*, 2009, **48**, 307-318.
48 69 A. S. Novikov, M. L. Kuznetsov, A. J. L. Pombeiro, N. A. Bokach and G. B. Shul'pin, *ACS*
49 *Catal.*, 2013, **3**, 1195-1208.
50
51
52
53
54
55
56
57
58
59
60

- 1
2 70 M. L. Kuznetsov, F. A. Teixeira, N. A. Bokach, A. J. L. Pombeiro and G. B. Shul'pin, *J. Catal.*,
3 2014, **313**, 135-148.
4 71 B. G. M. Rocha, M. L. Kuznetsov, Y. N. Kozlov, A. J. L. Pombeiro and G. B. Shul'pin, *Catal.*
5 *Sci. Technol.*, 2015, **5**, 2174-2187.
6 72 D. Dragancea, N. Talmaci, S. Shova, G. Novitchi, D. Darvasiová, P. Rapta, M. Breza, M.
7 Galanski, J. Kožíšek, N. M. R. Martins, L. M. D. R. S. Martins, A. J. L. Pombeiro and V. B. Arion,
8 *Inorg. Chem.*, 2016, **55**, 9187-9203.
9 73 I. Gryca, K. Czerwińska, B. Machura, A. Chrobok, L. S. Shul'pina, M. L. Kuznetsov, D. S.
10 Nesterov, Y. N. Kozlov, A. J. L. Pombeiro, I. A. Varyan and G. B. Shul'pin, *Inorg. Chem.*, 2018,
11 **57**, 1824-1839.
12 74 Bruker, *APEX2 & SAINT*; AXS Inc.: Madison, WI, 2004.
13 75 A. Altomare, M. C. Burla, M. Camalli, G. L. Casciaro, C. Giacovazzo, A. Guagliardi, A. G. G.
14 Moliterni, G. Polidori and R. Spagna, *J. Appl. Cryst.*, 1999, **32**, 115-119.
15 76 G. M. Sheldrick, *Acta Cryst.*, 2015, **C71**, 3-8, <https://doi.org/10.1107/S2053229614024218>.
16 77 L. J. Farrugia, *J. Appl. Cryst.*, 2012, **45**, 849-854.
17 78 A. L. Spek, *Acta Crystallogr., Sect. C*, 2015, **71**, 9-18.
18 79 Y. Zhao and D. G. Truhlar, *Theor. Chem. Acc.* 2008, **120**, 215-241.
19 80 M. J. Frisch, G. W. Trucks, H. B. Schlegel, G. E. Scuseria, M. A. Robb, J. R. Cheeseman, G.
20 Scalmani, V. Barone, B. Mennucci, G. A. Petersson, H. Nakatsuji, M. Caricato, X. Li, H. P.
21 Hratchian, A. F. Izmaylov, J. Bloino, G. Zheng, J. L. Sonnenberg, M. Hada, M. Ehara, K. Toyota,
22 R. Fukuda, J. Hasegawa, M. Ishida, T. Nakajima, Y. Honda, O. Kitao, H. Nakai, T. Vreven, J. A.,
23 Jr. Montgomery, J. E. Peralta, F. Ogliaro, M. Bearpark, J. J. Heyd, E. Brothers, K. N. Kudin, V. N.
24 Staroverov, R. Kobayashi, J. Normand, K. Raghavachari, A. Rendell, J. C. Burant, S. S. Iyengar, J.
25 Tomasi, M. Cossi, N. Rega, J. M. Millam, M. Klene, J. E. Knox, J. B. Cross, V. Bakken, C. Adamo,
26 J. Jaramillo, R. Gomperts, R. E. Stratmann, O. Yazyev, A. J. Austin, R. Cammi, C. Pomelli, J. W.
27 Ochterski, R. L. Martin, K. Morokuma, V. G. Zakrzewski, G. A. Voth, P. Salvador, J. J.
28 Dannenberg, S. Dapprich, A. D. Daniels, Ö. Farkas, J. B. Foresman, J. V. Ortiz, J. Cioslowski and
29 D. J. Fox, Gaussian, Inc., Wallingford CT, Gaussian 09, Revision A.01, Wallingford CT
30 81 M. Dolg, U. Wedig, H. Stoll and H. Preuss, *J. Chem. Phys.*, 1987, **86**, 866-872.
31 82 C. Gonzalez and H. B. Schlegel, *J. Chem. Phys.*, 1991, **95**, 5853-5860.
32 83 C. Gonzalez and H. B. Schlegel, *J. Chem. Phys.*, 1989, **90**, 2154-2161.
33 84 C. Gonzalez and H. B. Schlegel, *J. Phys. Chem.*, 1990, **94**, 5523-5527.
34 85 J. Tomasi and M. Persico, *Chem. Rev.*, 1994, **94**, 2027-2094.
35 86 V. Barone and M. Cossi, *J. Phys. Chem. A*, 1998, **102**, 1995-2001.
36 87 G. H. Wertz, *J. Am. Chem. Soc.*, 1980, **102**, 5316-5322.
37 88 J. Cooper and T. Ziegler, *Inorg. Chem.*, 2002, **41**, 6614-6622.
38
39
40
41
42
43
44
45
46
47
48
49
50
51
52
53
54
55
56
57
58
59
60

Table of Contents

View Article Online
DOI: 10.1039/C9NJ00348G

Catalytic activities of oxidovanadium(V) complexes towards microwave-assisted peroxidative oxidation of cyclohexane and cyclohexanol are explored by experimental and DFT calculations.

